J Clin Immunol
DOI 10.1007/s10875-016-0351-9

LETTER TO EDITOR

AD Hyper-IgE Syndrome Due to a Novel Loss-of-Function Mutation in *STAT3*: a Diagnostic Pursuit Won by Clinical Acuity

Leen Moens[1] · Heidi Schaballie[2,3] · Barbara Bosch[3,4] · Arnout Voet[5] · Xavier Bossuyt[1] · Jean-Laurent Casanova[4,6,7,8,9] · Stephanie Boisson-Dupuis[4,7,10] · Stuart G. Tangye[11,12] · Isabelle Meyts[2,3]

Received: 23 August 2016 / Accepted: 31 October 2016
© Springer Science+Business Media New York 2016

Keywords Autosomal dominant hyper-IgE syndrome · STAT3 · unconventional T cells · autism

Abbreviations

AD-HIES	Autosomal dominant hyper-IgE syndrome
iNKT	Invariant natural killer T cells
MAIT	Mucosal-associated invariant T cells
STAT3	Signal transducer and activator of transcription 3
cTfh	Circulating follicular helper T cells

To the Editor

Autosomal dominant hyper-IgE syndrome (AD-HIES) is a primary immunodeficiency characterized by severe eczema, elevated serum IgE levels, and increased susceptibility to infection with *Staphylococcus aureus* and *Candida albicans* [1]. Typical non-immunologic features include joint hyperflexibility, delayed shedding of deciduous teeth, fractures due to minor trauma, and vascular anomalies. AD-HIES is caused by dominant-negative mutations predominantly in the DNA binding and Src homology 2 (SH2) domain of signal transducer and activator of transcription 3 (*STAT3*) [1–5]. Previously named Job's syndrome, the syndrome took

Leen Moens, Heidi Schaballie and Barbara Bosch contributed equally to this work.

Electronic supplementary material The online version of this article (doi:10.1007/s10875-016-0351-9) contains supplementary material, which is available to authorized users.

✉ Isabelle Meyts
Isabelle.Meyts@uzleuven.be

[1] Laboratory Medicine, Experimental Laboratory Immunology, Department of Laboratory Medicine, University Hospitals Leuven and KU Leuven, Leuven, Belgium

[2] Department of Immunology and Microbiology, Childhood Immunology, University Hospitals Leuven and KU Leuven, Leuven, Belgium

[3] Department of Pediatrics, University Hospitals Leuven, Leuven, Belgium

[4] St. Giles Laboratory of Infectious Diseases, Rockefeller Branch, The Rockefeller University, New York, NY, USA

[5] Department of Biochemistry, Laboratory of Biomolecular Modelling and Design, KU Leuven, Leuven, Belgium

[6] The Howard Hughes Medical Institute, New York, NY, USA

[7] The Laboratory of Human Genetics of Infectious Diseases, Necker Branch, INSERM U1163, Necker Hospital for Sick Children, Paris, France

[8] The Imagine Institute, Paris Descartes University, Paris, France

[9] The Pediatric Hematology and Immunology Unit, Assistance Publique-Hôpitaux de Paris, Necker Hospital for Sick Children, Paris, France

[10] Paris Descartes University, Imagine Institute, Paris, France

[11] Immunology Division, Garvan Institute of Medical Research, Darlinghurst, Australia

[12] St Vincent's Clinical School, University of NSW Australia, Darlinghurst, Australia

Published online: 14 November 2016

its name from the finding of marked elevation of polyclonal serum IgE. The STAT3-HIES clinical phenotype score in patients with elevated IgE serum levels (>1000 IU/mL) summarizes the main clinical and laboratory findings in AD-HIES (score >40) and facilitates early diagnosis of AD-HIES and thus initiation of appropriate therapy [6].

IgE levels vary in AD-HIES over time with lower levels in infancy, elevated levels in childhood, and declining levels in adults [1]. The pathophysiology of the elevated IgE is still incompletely understood: it is unclear whether the explanation lies in the requirement for STAT3 signaling in the B cell or in the T cells providing help to B cells in the antibody response [7]. Recent work by Kane et al. used conditional loss of STAT3 in B cells to show that deficiency of STAT3 in B cells alone recapitulates the aberrantly elevated IgE level, at least in the setting of a murine model of complete STAT3 deficiency [8]. Elevated serum IgE levels are neither essential nor sufficient for the diagnosis of AD-HIES as: (i) singular cases of AD-HIES with normal serum IgE in early childhood have been described and (ii) the finding of elevated serum IgE can lead to incorrect phenotypical diagnosis of AD-HIES [9, 10].

Numerous cellular defects have been reported in AD-HIES, and several of these contribute to disease pathogenesis. A lack of Th17 cells is central to the pathogenesis of candidiasis and perhaps staphylococcal infection in patients with AD-HIES [11]. Lack of IL-17-mediated immunity is key to the development of chronic mucocutaneous candidiasis and to a lesser extent recurrent staphylococcal infection in various PIDs [12–17]. Ma et al. demonstrated that signaling through STAT3 downstream of the IL23R is required for Th17 development [17]. Patients with LOF mutations in *STAT3* have reduced numbers of T follicular helper cells (Tfh) ex vivo as evidenced by decreased proportions of circulating CD4(+)CD45RO(+)CXCR5(+)T cells [7]. Moreover, Deenick and Tangye described reduced numbers of invariant Natural Killer T (iNKT) and mucosal-associated invariant T (MAIT) cells yet normal γδ T cells in AD-HIES, pointing to a role for STAT3 signaling in the generation and/or maintenance of these innate-type T cells [18].

We present a molecular diagnosis of a missense mutation in *STAT3* in an 8-year-old boy with normal serum IgE levels. The report is compelling for several reasons. First, we describe a novel mutation in the DNA-binding domain of *STAT3*. Second, although the immunological and non-immunological phenotypes were explicit and severe, the absence of elevated IgE and the presence of autism led to a delay in diagnosis and treatment. Finally, we report the patient's normal numbers of iNKT cells and MAIT cells yet elevated γδ TCR T cells expressing predominantly Vδ1. This report highlights the power of clinical acuity and the relevance of pursuing a molecular diagnosis even if the laboratory values do not add up.

Case Description

An 8-year-old boy born to non-consanguineous parents of Flemish descent was admitted with *S. aureus* sepsis and pleuropneumonia. His past medical history was noteworthy with severe eczema from birth and extensive diaper dermatitis. Other medical concerns included mucocutaneous candidiasis, frequent upper and lower respiratory tract infections from birth, gingivitis and stomatitis, and six episodes of typical febrile seizures prior to the age of 4. Extraction of three primary teeth was necessary to allow for normal eruption of permanent teeth. His wrist was fractured twice after minor trauma. He was diagnosed with autism-spectrum disorder at age 5. Because of autism with mild dysmorphic features, Beckwith-Wiedemann syndrome (OMIM 130650), Coffin-Lowry syndrome (OMIM 303600), and ATR-X syndrome (OMIM 300032) were excluded by Sanger sequencing.

Basic immunological work-up was normal (Table SI). Upon the first visit to the pediatric primary immunodeficiency clinic, AD-HIES was suspected. However, serum IgE level was normal at 180 IU/mL. More extensive analysis showed low switched memory B cells (compatible with but not specific for AD-HIES) and high CD3(+) γδTCR(+) T cells (+/− 20% of CD3(+) cells). The anti-polysaccharide antibody response to unconjugated pneumococcal vaccine was normal. The NIH score for HIES and STAT3-HIES were both 42 (probable AD-HIES) [1, 6]. Sanger sequencing of *STAT3* showed a heterozygous variant: g.40485745T>G resulting in the replacement of a highly conserved histidine amino acid at position 332 in the DNA-binding domain of STAT3 by proline (H332P; Figure S1, S2). This variant was not found in public databases. Polyphen2 score is 0.995 (probably damaging), and SIFT score is 0.051 (tolerated). CADD score (NC_000017.10 g.40485745T>G, NM_003150.3 c.995T>G) (Ensembl genome browser 75 public database; Assembly GRC37/hg19) is 25.9 and MSC for CADD is 15.290. The amino acid at position 332 is conserved throughout species (Figure S3). The substitution occurred de novo, as it was absent in both parents (data not shown).

We studied the functional impact of the H332P substitution. Tyrosine phosphorylation of STAT3 at position 705 after IL-21 stimulation was intact in the index patient (see Online Supplement for Materials and Methods; Figure S3). Binding of H332P STAT3 to DNA was decreased compared to the control; similar results were observed for STAT3 from patients with previously confirmed pathogenic mutations. Functionally, STAT3-dependent inhibition of LPS-induced TNF-α production mediated by IL-10 in monocyte-derived macrophages was abolished in the patient compared to a healthy control [6] (see Online Supplement for Materials and Methods; Fig. 1) confirming the LOF effect of the mutation. The impact of the p.H332P mutation on the crystal structure of STAT3 is shown in Fig. 2. Amino acid position 332 is situated

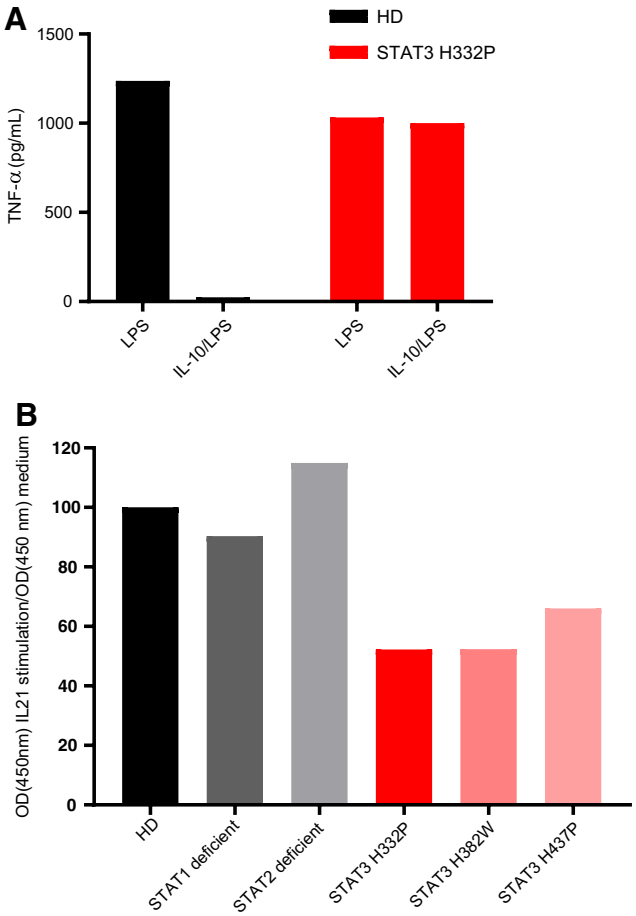

Fig. 1 Binding of H332P STAT3 to DNA (*upper panel*) and STAT3-dependent inhibition of LPS-induced TNF-α production (*lower panel*). **a** STAT3-dependent DNA-binding capacity of nuclear extracts as ratio of OD (450 nm) of IL21-stimulated condition over OD (450 nm) of the unstimulated condition for STAT3 WT LCL (control), STAT3 H332P LCL (patient), and two LCLs with confirmed STAT3 mutations in the DNA-binding domain (H382W and H437P) (TransAm STAT3). **b** STAT3 dependent IL-10-mediated inhibition of LPS-induced TNF-α production by monocyte-derived macrophages from control individuals (STAT3 WT, $n = 3$) and AD-HIES patient (H332P STAT3). Presented is the TNF-α release after LPS stimulation with or without addition of IL-10

in the core of the DNA binding domain in the vicinity of an asparagine residue at position 466, which binds the DNA sequence (Fig. 2a) [19]. The positively charged H332 forms a salt bridge with the negatively charged phosphate backbone of the DNA helix. The H332P mutation disrupts this salt bridge, thereby hampering the interaction with the DNA strand (Fig. 2b).

The percentage of IL-17A-producing CD4(+)CD45RA(−)T cells following *S. aureus* enterotoxin B stimulation was significantly decreased in the index patient and two additional STAT3 deficient AD-HIES patients with known pathogenic mutations compared to healthy donors ($p = 0.017$) (Fig. 3a, b). In IL-17A secretion after stimulation with PHA, heat-inactivated *C. albicans* and *S. aureus* was low (Fig. 3c, d) whereas IFN-γ secretion was normal. The percentage of Tfh cells was decreased in the index patient and in confirmed AD-HIES patients compared to healthy individuals ($p = 0.024$, Fig. 3e). There was a predominance of Vδ1+ T cells (7.6% of CD3(+) cells) in the index patient (Fig. 3f) and he had normal numbers of iNKT cell and MAIT cells (Fig. 3g, h).

Discussion

This report highlights several aspects of PID in general and AD-HIES in particular. First, the infectious phenotype of the described patient was highly suggestive of a PID, specifically AD-HIES. Nevertheless, the patient only came to our attention after he had been admitted to a tertiary care hospital with *S. aureus* sepsis. The NIH score and adapted STAT3 HIES score were both predictive of a *STAT3* mutation. We identified a novel mutation in the DNA-binding domain of STAT3 (H332P) and validated it by analyzing its effect on DNA binding and on cytokine production. Different amino acid substitutions at the same position have previously been reported (H332Y, H332L) [20]. This case highlights the high sensitivity of the clinical phenotype of AD-HIES to detect a *STAT3* loss of function mutation, independent of the level of IgE. Especially in children, investigations for AD-HIES should not be delayed because of normal IgE. At least two other pediatric cases of AD-HIES with normal IgE have been described (2 months and 7 years of age) [10]. By the age of 8, both children had IgE levels above 1000 kU/L (personal communication, Chandesris and Picard). The cases reported with the H332Y and H332L STAT3 mutations had elevated IgE (>1000 kU/L) suggesting that the normal IgE in the index patient is not a feature of the novel mutation (personal communication, E Renner). The normal IgE in this report is therefore surprising and unexplained.

Second, the presence of autism and mild developmental delay combined with some dysmorphic features had led to referral to clinical genetics and multiple diagnostic Sanger sequencing runs, diverting attention from the obvious infectious phenotype. One patient with AD-HIES and autism has previously been reported [21–24]. Several PIDs are associated with developmental delay and autism-spectrum disorders, e.g., Di George syndrome, Coronin1A deficiency, and GATA2 deficiency [22–24]. In light of this especially in children, a diagnosis of autism and presence of dysmorphic features cannot be uncoupled from the infectious phenotype and a genetic diagnosis explaining the entire phenotype should be sought. This has important therapeutic implications: in the index case, adequate antibiotic and antifungal prophylaxis led to excellent control of infections with an important functional impact on the child's behavior both at school and at home.

Third, an essential role for STAT3 signaling in controlling unconventional T cell number and function was recently

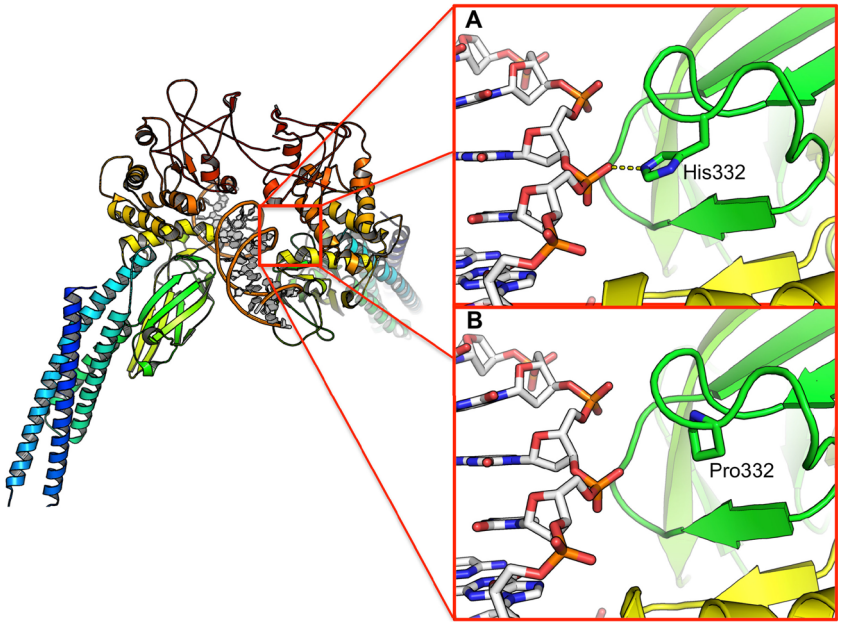

Fig. 2 The influence of the H332P mutation on the crystal structure of STAT3 and its impact on DNA binding. The STAT3 dimer bound to DNA is represented as a cartoon (*blue* to *red* for N to C termini) on the left side. **a** depicts the zoom in on the wild-type structure in which the positively charged His332 binds the negative phosphate backbone of the DNA represented by the *dashed yellow lines* (salt bridge). **b** In the mutant structure, this salt bridge is lost, hampering the interaction with the DNA strand

identified [18]. The index patient has normal numbers of iNKT cells and MAIT cells. We identified another STAT3 deficient patient (G617V) with normal iNKT and MAIT cell numbers in our cohort (unpublished observation). However, another AD-HIES patient included as a positive control showed low numbers of these cells, in accordance with earlier findings [18]. These findings stress the variability in unconventional T cell numbers in AD-HIES. Interestingly, the index patient has high numbers of Vδ1+ cells, which usually constitute a minority of blood γδ TCR T cells [25]. We hypothesize that the peripheral blood expansion of Vδ1+ T cells in this patient results from chronic infection with *Candida* sp.

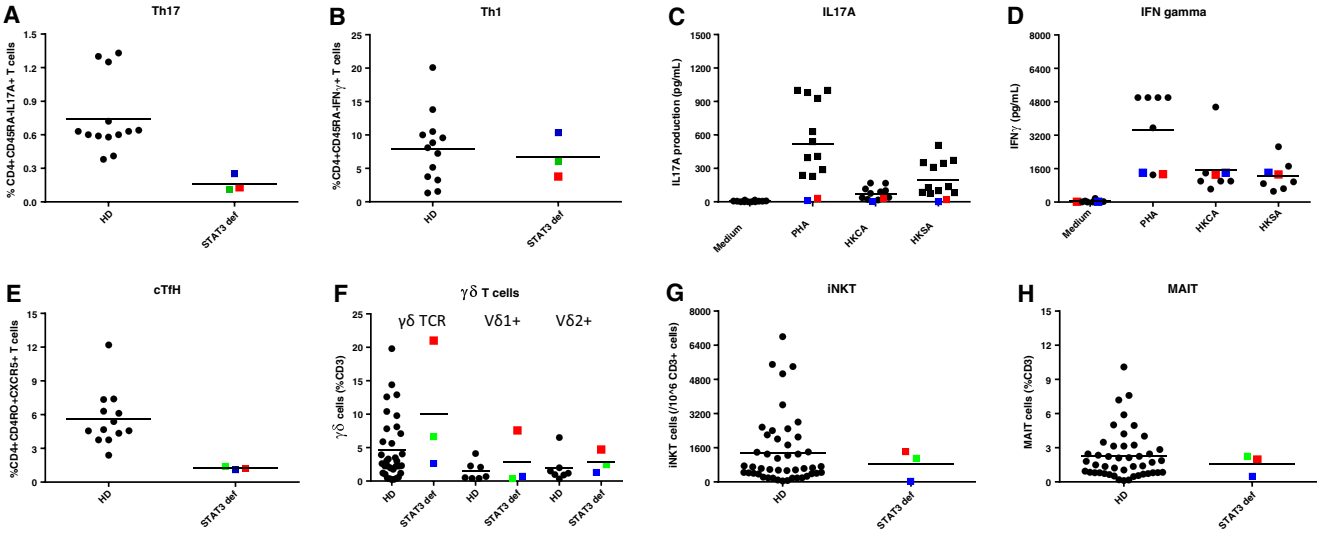

Fig. 3 Th17 cells, in vitro IL-17A production, cTfh and unconventional T cells in the index patient, and patients with AD-HIES due to confirmed LOF mutations in STAT3 and healthy donors. **a**, **b** Percentage IL-17A (**a**) and IFN-γ producing CD4(+) CD45RA(−) T cells (**b**) from healthy donors, not carrying mutations in *STAT3* (*black symbols*; $n = 13$), the index patient (H332P, *red symbol*), and two AD-HIES patients with confirmed pathogenic LOF mutations in *STAT3* [*green symbol* (G617V); *blue symbol* (Y705H)]. **c**, **d** IL-17A (**c**) and IFN-γ (**d**) production (pg/mL) by PBMC from healthy donors (*black symbols*; $n = 6$–11), compared to the index patient (*red symbol*) and one AD-HIES patient with confirmed pathogenic LOF mutation in *STAT3* (Y705H (*blue symbol*)) after stimulation with medium, phytohaemagglutinin (PHA), heat-inactivated *Candida albicans* (HKCA) and heat-inactivated *S. aureus* (HKSA) as measured by ELISA. **e** Percentage of cTfh cells [CD4(+)CD45RO(+)CXCR5(+) T cells] from healthy donors ($n = 5$, WT) the index patient (H332P, *red mark*) and two AD-HIES patients with confirmed pathogenic LOF mutations in *STAT3*. **f** Flow cytometric quantification of γδ TCR T cells, Vδ1+ TCR T cells, and Vδ2+ TCR T cells. **g** Flow cytometric quantification of iNKT cells in the index patient, two patients with AD-HIES and healthy donors (HD) ($n = 46$). **h** Flow cytometric quantification of MAIT cells in the index patient, two patients with AD-HIES and healthy donors (HD) ($n = 46$)

Interestingly, the two other STAT3+/− patients had no documented or reported *Candida* infection. Two recent papers demonstrate that in HIV patients with candidiasis Vδ1+ T cells are important sources of IL-17 [26, 27]. More research is needed on the function of γδ TCR T, MAIT, and iNKT cells in conditions of Th17 deficiency, especially since these unconventional T cells have been implicated in recognition of *S. aureus* and *C. albicans*, two key pathogens in AD-HIES.

In conclusion, we report a novel loss-of-function mutation in *STAT3* in a patient with a typical clinical phenotype of AD-HIES yet with normal serum IgE. Although elevated IgE is a hallmark of the disease, it is not essential for the diagnosis of AD-HIES. Moreover, the patient displays increased γδ T cell numbers in the peripheral blood as well as normal NKT and MAIT cells adding to the mystery of unconventional T cells in monogenic PID syndromes. Finally, even in the era of next generation sequencing, clinical acuity sometimes prevails: in the absence of clear biochemical or immunological (in the sense of hematological) phenotype, the diagnostic pathway should be followed including molecular diagnosis if the clinical phenotype is strongly suggestive of a particular PID.

Acknowledgements The authors thank Olivia Chandesris, Capucine Picard, and Ellen Renner for sharing follow-up information on their AD-HIES cohort.

Compliance with Ethical Standards

Funding IM is funded by a KOF mandate of the KU Leuven, by an International Mobility Grant of the FWO Vlaanderen and by the Jeffrey Modell Foundation, HS and BB are funded by a Research Mandate of the FWO Vlaanderen, and XB is funded by a research grant of the Research Council of the Catholic University of Leuven.

Conflict of Interest The authors declare that they have no conflict of interest.

References

1. Holland SM, DeLeo FR, Elloumi HZ, Hsu AP, Uzel G, Brodsky N, et al. STAT3 mutations in the hyper-IgE syndrome. N Engl J Med. 2007;357(16):1608–19.
2. Minegishi Y, Saito M, Tsuchiya S, Tsuge I, Takada H, Hara T, et al. Dominant-negative mutations in the DNA-binding domain of STAT3 cause hyper-IgE syndrome. Nature. 2007;448(7157):1058–62.
3. Vogel TP, Milner JD, Cooper MA. The ying and yang of STAT3 in human disease. J Clin Immunol. 2015;35(7):615–23.
4. Hagl B, Heinz V, Schlesinger A, Spielberger BD, Sawalle-Belohradsky J, Senn-Rauh M, et al. Key findings to expedite the diagnosis of hyper-IgE syndromes in infants and young children. Pediatr Allergy Immunol. 2016;27(2):177–84.
5. Schimke LF, Sawalle-Belohradsky J, Roesler J, Wollenberg A, Rack A, Borte M, et al. Diagnostic approach to the hyper-IgE syndromes: immunologic and clinical key findings to differentiate hyper-IgE syndromes from atopic dermatitis. J Allergy Clin Immunol. 2010;126(3):611–7 e1.
6. Woellner C, Gertz EM, Schaffer AA, Lagos M, Perro M, Glocker EO, et al. Mutations in STAT3 and diagnostic guidelines for hyper-IgE syndrome. J Allergy Clin Immunol. 2010;125(2):424–32 e8.
7. Ma CS, Avery DT, Chan A, Batten M, Bustamante J, Boisson-Dupuis S, et al. Functional STAT3 deficiency compromises the generation of human T follicular helper cells. Blood. 2012;119(17):3997–4008.
8. Kane A, Lau A, Brink R, Tangye SG, Deenick EK. B-cell-specific STAT3 deficiency: Insight into the molecular basis of autosomal-dominant hyper-IgE syndrome. J Allergy Clin Immunol. 2016;S0091–6749(16):30437–7.
9. Frans G, Moens L, Schrijvers R, Wuyts G, Bouckaert B, Schaballie H, et al. PID in disguise: molecular diagnosis of IRAK-4 deficiency in an adult previously misdiagnosed with autosomal dominant hyper IgE syndrome. J Clin Immunol. 2015;35(8):739–44.
10. Chandesris MO, Melki I, Natividad A, Puel A, Fieschi C, Yun L, et al. Autosomal dominant STAT3 deficiency and hyper-IgE syndrome: molecular, cellular, and clinical features from a French national survey. Medicine (Baltimore). 2012;91(4):e1–e19.
11. Ma CS, Chew GY, Simpson N, Priyadarshi A, Wong M, Grimbacher B, et al. Deficiency of Th17 cells in hyper IgE syndrome due to mutations in STAT3. J Exp Med. 2008;205(7):1551–7.
12. Ling Y, Cypowyj S, Aytekin C, Galicchio M, Camcioglu Y, Nepesov S, et al. Inherited IL-17RC deficiency in patients with chronic mucocutaneous candidiasis. J Exp Med. 2015;212(5):619–31.
13. Boisson B, Wang C, Pedergnana V, Wu L, Cypowyj S, Rybojad M, et al. An ACT1 mutation selectively abolishes interleukin-17 responses in humans with chronic mucocutaneous candidiasis. Immunity. 2013;39(4):676–86.
14. Okada S, Markle JG, Deenick EK, Mele F, Averbuch D, Lagos M, et al. Immunodeficiencies. Impairment of immunity to Candida and Mycobacterium in humans with bi-allelic RORC mutations. Science. 2015;349(6248):606–13.
15. Liu L, Okada S, Kong XF, Kreins AY, Cypowyj S, Abhyankar A, et al. Gain-of-function human STAT1 mutations impair IL-17 immunity and underlie chronic mucocutaneous candidiasis. J Exp Med. 2011;208(8):1635–48.
16. Marodi L, Cypowyj S, Toth B, Chernyshova L, Puel A, Casanova JL. Molecular mechanisms of mucocutaneous immunity against Candida and Staphylococcus species. J Allergy Clin Immunol. 2012;130(5):1019–27.
17. Ma CS, Wong N, Rao G, Nguyen A, Avery DT, Payne K, et al. Unique and shared signaling pathways cooperate to regulate the differentiation of human CD4+ T cells into distinct effector subsets. J Exp Med. 2016;213(8):1589–608.
18. Wilson RP, Ives ML, Rao G, Lau A, Payne K, Kobayashi M, et al. STAT3 is a critical cell-intrinsic regulator of human unconventional T cell numbers and function. J Exp Med. 2015;212(6):855–64.
19. Nkansah E, Shah R, Collie GW, Parkinson GN, Palmer J, Rahman KM, et al. Observation of unphosphorylated STAT3 core protein binding to target dsDNA by PEMSA and X-ray crystallography. FEBS Lett. 2013;587(7):833–9.
20. Jiao H, Toth B, Erdos M, Fransson I, Rakoczi E, Balogh I, et al. Novel and recurrent STAT3 mutations in hyper-IgE syndrome patients from different ethnic groups. Mol Immunol. 2008;46(1):202–6.
21. Grimbacher B, Dutra AS, Holland SM, Fischer RE, Pao M, Gallin JI, et al. Analphoid marker chromosome in a patient with hyper-IgE syndrome, autism, and mild mental retardation. Genet Med. 1999;1(5):213–8.
22. Wlodarski MW, Hirabayashi S, Pastor V, Stary J, Hasle H, Masetti R, et al. Prevalence, clinical characteristics, and prognosis of GATA 2-related myelodysplastic syndromes in children and adolescents. Blood. 2016;127(11):1387–97.

23. Shiow LR, Paris K, Akana MC, Cyster JG, Sorensen RU, Puck JM. Severe combined immunodeficiency (SCID) and attention deficit hyperactivity disorder (ADHD) associated with a Coronin-1A mutation and a chromosome 16p11.2 deletion. Clin Immunol. 2009;131(1):24–30.
24. Tang KL, Antshel KM, Fremont WP, Kates WR. Behavioral and psychiatric phenotypes in 22q11.2 deletion syndrome. J Dev Behav Pediatr. 2015;36(8):639–50.
25. Godfrey DI, Uldrich AP, McCluskey J, Rossjohn J, Moody DB. The burgeoning family of unconventional T cells. Nat Immunol. 2015;16(11):1114–23.
26. Maher CO, Dunne K, Comerford R, O'Dea S, Loy A, Woo J, et al. Candida albicans stimulates IL-23 release by human dendritic cells and downstream IL-17 secretion by Vdelta1 T cells. J Immunol. 2015;194(12):5953–60.
27. Fenoglio D, Poggi A, Catellani S, Battaglia F, Ferrera A, Setti M, et al. Vdelta1 T lymphocytes producing IFN-gamma and IL-17 are expanded in HIV-1-infected patients and respond to Candida albicans. Blood. 2009;113(26):6611–8.

Supplemental Materials and Methods

Determination of STAT3 phosphorylation

Freshly thawn PBMCs were incubated with 100 ng IL-21 (eBioscience) for 15 min at 37°C, followed by 10 min fixation with 2% formaldehyde at room temperature. Anti-CD3 APC eFluor 780 (eBioscience), anti-CD4 APC (eBioscience) and anti-CD19 Brilliant violet 421 (BioLegend) were added 15 min before the IL-21 for surface staining for a total of 30 min. Samples were washed twice by centrifugation using PBS containing 2% heat inactivated FCS, then permeabilized with 80% ice cold methanol for 30 minutes. pSTAT3 Alexa Fluor488 (BD) was then added and incubated at 4°C overnight. The samples were run the next day on the Canto II and analyzed using Flowjo software.

IL-10 mediated inhibition of LPS stimulated TNF- α release

Monocyte derived macrophages were pre-incubated with human IL-10 (BD, 25 ng/mL) for one hour and then stimulated overnight with LPS (Sigma-Aldrich, 50ng/mL) as previously described (1). TNF-α concentration in the supernatant was measured by ELISA (BD Pharmingen).

Assessment of DNA binding activity of STAT3

Nuclear extracts from LCLs with or without IL-21 stimulation were prepared as described by the manufacturer (Active Motif Europe) and as previously described (2). Samples were used for detection and quantification of STAT3 dependent DNA binding by TransAm STAT3 ELISA (Active Motif Europe).

Crystal structure of STAT3 and effect of H332P on DNA binding

To investigate the influence of the H332P mutation on the STAT3 structure and interactions molecular modelling was performed. The dimeric STAT3 wild-type structure bound to DNA (PDB entry 4E68) was utilized (3). The mutation was introduced using MOE (The Chemical Computing group, Montreal, Canada), followed by energy-minimization of the structure in in a 5 A radius of amino acid position 332.

In vitro IL-17A production and Th17 differentiation; quantification of circulating Tfh, iNKT, MAIT and Vδ1 and Vδ2 T cells

IFN-γ (BD) and IL-17A (eBioscience) secretion post stimulation with PHA (Sigma-Aldrich), heat inactivated *C. albicans* (Invivogen) or heat inactivated *Staphylococcus aureus* (Invivogen) were measured by ELISA after 48h and 5 days, respectively.

Freshly thawed PBMCs were resuspended ($1x10^6$/mL) in RPMI containing 10%FCS were exposed to *Staphylococcus* enterotoxin B (Sigma-Aldrich, 1µg/mL) and Brefeldin A (eBioscience, 2.5µg/mL) for 16 hours at 37°C and 5% CO_2 (1). The cells were then surface stained for CD3 APC eFluor 780, CD4 APC and CD45RA PE Cy7, followed by an intracellular staining for IL-17A FITC and IFN-γ eFluor 450. All the antibodies were available from

eBioscience. Intracellular staining was performed by using Cytofix/cytoperm fixation/Permeabilization kit (BD Biosciences).

Numbers of circulating Tfh cells were evaluated by surface staining as described by Ma et al. (4). CD3 V500, CD4 APC-H7, and CXCR5 Alexa Fluor 647 were from BD Biosciences. CD19 Brilliant Violet and CD45RO FITC were available from BioLegend and eBioscience, respectively.

Cells were labeled according to standard protocols. iNKT cells were identified as CD19-CD3+Vα24+V β11+ cells with FITC anti-Vβ11 and PE-Cy7 anti-Vα24 from Beckman-Coulter. MAIT cells were stained with BV421 anti-CD161 and PerCP-Cy5.5 anti-Vα7.2 antibodies from Sony. Vδ1 and Vδ2 T cells were stained with Vδ1-APC from Miltenyi and Vδ2-FITC from BD. At least $1x10^6$ events were collected in the CD3 gate. Samples were acquired on a FACS Fortessa (BD Biosciences). Data were analyzed using FlowJo software Version 10.1 (Treestar).

Table SI Peripheral blood values and immunophenotyping at diagnosis (age 8)

	Patient	**Age-specific Reference value**
Hemoglobin	11.8 g/dL	11.5-15.5
Thrombocytes	199 x 10*9/L	150-450
White blood cells	4.93 x 10*9/L	4.5-13.5
Neutrophils	2.8 x 10*9/L	1.8-8.0
Basophils	0.0 x 10*9/L	<0.1
Lymphocytes	2.7 x 10*9/L	1.5-6.5
Monocytes	0.6 x 10*9/L	> 0.4
Eosinophils	0,1 x 10*9/L	< 0,3
IgG	11 g/L	5.58-12.54
IgA	0.91 g/L	0.29-3.84
IgM	1.08 g/L	0.34-1.42
IgE	180 kU/L	< 330

Absolute lymphocytosis	2.662 x 10*9/L	1100-5900
CD19(+) B lymphocytes	0.258 x 10*9/L	0.200 - 1.600
CD27(+)IgM(+)IgD(+)	7.5 % of B cells	7.5-12.4%
CD27(+)IgM(-)IgD(-)	2.7 % of B cells ↓	5.2-12.1%
CD27(-)IgM(+)IgD(+)	84.9 % of B cells ↑	69.4-80.4%
CD3(+) T cells	1.937 x 10*9/L	0.700 - 4.200
CD3(+)CD4(+) T cells	0.877 x 10*9/L	0.300 - 2.000
CD3(+)CD8(+) T cells	0.623 x 10*9/L	0.300 - 1.800
CD3(-)/CD56 and/or CD16(+) NK cells	0.459 x 10*9/L	0.090 - 0.900
CD3(+)CD27(+) CD45RA(+)	53.4%	45-90
CD3(+) gammadelta TCR cells	22.1% of CD3 ↑	<10%
Vδ1+ CD3+ cells	7.6% of CD3 ↑	1.5 (0.4 – 4.1)
Vδ2+ CD3+ cells	4.7% of CD3	1.9 (0.3 -6.5)
iNKT cells (/10*6 CD3+ cells)	1400	1373 (48 – 6762)
MAIT (% of CD3+ cells)	1.95	2.28 (0.14 – 9.08)
Lymphocyte proliferation in response to PHA stimulation	138640 cpm	>30000 cpm

Figure Legends

Figure S1:

***STAT3* sequencing data of DNA fragment at nucleotide position c.996A>C from control individual (above) and index patient (below).**

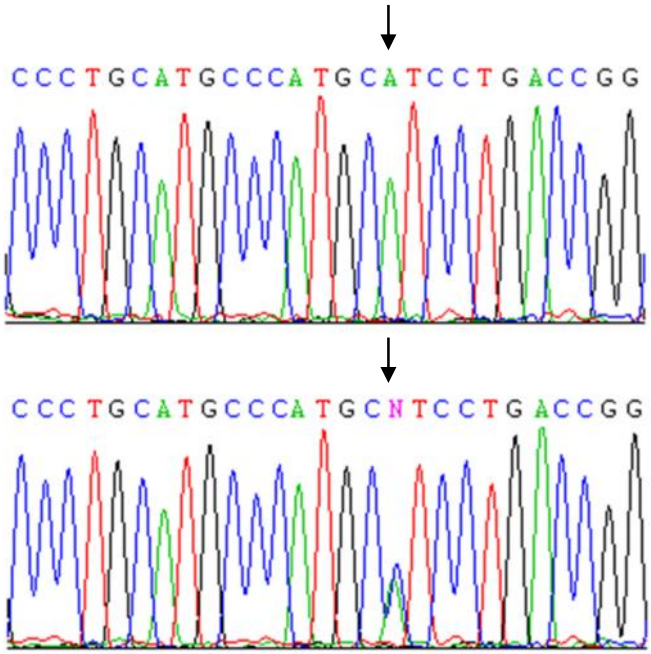

Figure S2. The amino acid position 332 is conserved throughout species

H. sapiens	NP_644805.1	305	LEERIVELFRNLMKSAFVVERQPCMPMHPDRPLVIKTGVQFTTKVRLLVK	354
P. troglodytes	XP_001165417.2	399	LEERIVELFRNLMKSAFVVERQPCMPMHPDRPLVIKTGVQFTTKVRLLVK	448
M. mulatta	XP_002800523.1	399	LEERIVELFRNLMKSAFVVERQPCMPMHPDRPLVIKTGVQFTTKVRLLVK	448
C. lupus	XP_005624514.1	305	LEERIVELFRNLMKSAFVVERQPCMPMHPDRPLVIKTGVQFTTKVRLLVK	354
B. taurus	NP_001012689.2	305	LEERIVELFRNLMKSAFVVERQPCMPMHPDRPLVIKTGVQFTTKVRLLVK	354
M. musculus	NP_998824.1	305	LEERIVELFRNLMKSAFVVERQPCMPMHPDRPLVIKTGVQFTTKVRLLVK	354
R. norvegicus	NP_036879.1	305	LEERIVDLFRNLMKSAFVVERQPCMPMHPDRPLVIKTGVQFTTKVRLLVK	354
G. gallus	NP_001026102.1	305	LEERIVELFRNLMKSAFVVERQPCMPMHPDRPLVFKTGVQFTTKVRLLVK	354
X. tropicalis	NP_571554.1	306	LEEKIVDLFRNLMKSAFVVERQPCMPMHPDRPLVIKTGVQFTTKVRLLVK	355
D. rerio	XP_002941970.2	229	LEERIVELFRNLMKSAFVVERQPCMPMHPDRPLVIKTGVQFTTKVRLLVK	278

Figure S2.

Figure S3.

Tyrosine phosphorylation status of CD4(+) T cells in STAT3 wildtype and mutant individuals (H332P in red) after IL-21 stimulation, expressed as the ratio of mean fluorescence intensity (MFI) of the IL-21 stimulated condition over the MFI of the unstimulated condition.

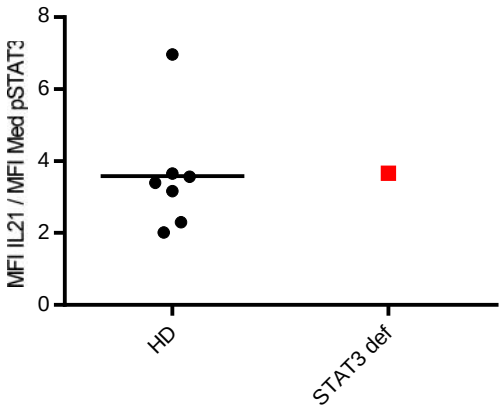

References

1. Woellner C, Gertz EM, Schaffer AA, Lagos M, Perro M, Glocker EO, et al. Mutations in STAT3 and diagnostic guidelines for hyper-IgE syndrome. J Allergy Clin Immunol. 2010;125(2):424-32 e8.
2. Pelham SJ, Lenthall HC, Deenick EK, Tangye SG. Elucidating the effects of disease-causing mutations on STAT3 function in autosomal-dominant hyper-IgE syndrome. J Allergy Clin Immunol. 2016.
3. Nkansah E, Shah R, Collie GW, Parkinson GN, Palmer J, Rahman KM, et al. Observation of unphosphorylated STAT3 core protein binding to target dsDNA by PEMSA and X-ray crystallography. FEBS Lett. 2013;587(7):833-9.
4. Ma CS, Avery DT, Chan A, Batten M, Bustamante J, Boisson-Dupuis S, et al. Functional STAT3 deficiency compromises the generation of human T follicular helper cells. Blood. 2012;119(17):3997-4008.